A model for the prediction of structure–property relations in cross-linked polymers

Joel P. Foreman [a], David Porter [b], Shabnam Behzadi [a], Frank R. Jones [a],*

[a] Department of Engineering Materials, University of Sheffield, Mappin Street, Sheffield, S1 3JD, UK
[b] Department of Zoology, University of Oxford, South Parks Road, Oxford, OX1 3PS, UK

ARTICLE INFO

ABSTRACT

A model is presented that predicts the nonlinear mechanical properties of a highly cross-linked thermosetting polymer as a function of temperature, strain, and strain rate. The model is a significant extension of Group Interaction Modelling (GIM) that was originally developed for linear amorphous thermoplastics. Fundamental energy contributions within and between characteristic mer units are used to model the dynamic mechanical spectrum of the polymer. This enables the model to be applied to the prediction of the full stress–strain profile through yield. Tetraglycidyl 4,4′-diaminodiphenylmethane cured with 4,4′-diaminodiphenylsulphone is used as a detailed example for validation and the model predictions are in good agreement with experiment.

1. Introduction

Recently there has been renewed interest in developing modelling techniques to predict the properties of high performance structural polymers [1]. However, these polymers tend to rely on multifunctional components that create complex network structures where significant uncertainty exists over exact structural details. Therefore, a modelling technique that circumvents the need for such information and relies on a mean-field approach is required instead. The technique used in this work is Group Interaction Modelling (GIM) which has previously been successfully applied to a wide variety of linear polymers [2]. Its application to multifunctional-branched polymers is limited and the extra level of complexity has lead to previous efforts necessarily targeting one or two specific, isolated properties [3,4]. These earlier versions of the model have been significantly extended here so that a series of linked temperature dependent properties of a highly cross-linked polymer are predicted. In addition, the extended model is able to predict the temperature and strain rate dependence of the mechanical properties. To validate the model, the stress–strain curves through yield of a cured epoxy resin have been calculated and compared to equivalent experimental data.

The development of model systems capable of directly linking molecular structure to mechanical properties is driven by a need to limit the use of expensive experimental screening programs. Consequently, a variety of different techniques are currently being developed with this aim in mind. The models proposed by Lesser and Calzia [5,6] show a clear link between the molecular structure and yield behaviour of a number of cross-linking polymers. They use two specific parameters to characterise model trends based on the polymer stiffness (indicated by the glass transition temperature) and strength (cohesive energy). Their approach differs in how network formation is dealt with from that presented here. In this work, the molecular weight between cross-links is not required and a reduction in degrees of freedom per cross-link is used instead.

Amine cured epoxy resins are some of the most important matrices for fibre reinforced composite materials. The cured resins exhibit good strength, toughness, corrosion and moisture resistance, desirable thermal and electrical properties and minimal shrinkage [7]. Many commercial aerospace composite materials use diglycidyl ethers or multifunctional glycidyl amines, often as blends with one or more curing agents and a thermoplastic modifier to aid flow control and impart fracture toughness. One of the most common epoxies is tetraglycidyl 4,4′-diaminodiphenylmethane (TGDDM, sold as Araldite MY721) which has four highly reactive oxirane ring sites. A commonly used amine curing agent is 4,4′-diaminodiphenylsulphone (DDS) which ultimately also has four reactive amine sites.

The reaction of TGDDM with DDS is not a simple linear polymerisation. The tetrafunctional nature of both reactants leads to the formation of a highly cross-linked 3-D network. Whilst the curing mechanism is known [8], there exists considerable uncertainty over

* Corresponding author. Tel.: +44 114 222 5477; fax: +44 114 222 5943.
E-mail address: f.r.jones@sheffield.ac.uk (F.R. Jones).

the exact structure of any given amine cured epoxy resin and TGDDM/DDS is no exception. The two main reactions that occur are firstly a primary amine reacting with an epoxy group and secondly the resultant secondary amine also reacting with an epoxy group. A further reaction involving an opened and an unopened epoxy ring can occur but is considered to be less prevalent in TGDDM/DDS than in a similar trivalent epoxy system [9]. The reaction of any intermediate (e.g. a secondary amine or opened epoxy ring) creates a cross-link between two polymer chains and hence the network is formed.

In order to predict the mechanical properties of a fibre rein-forced composite, a hierarchical approach has been adopted [10] which starts by modelling the properties of the matrix. Finite element analysis [11] of the full composite system using the pre-dicted matrix properties is then used as the basis for a statistical model of fibre fracture [12]. This paper focuses on predicting the thermomechanical and engineering properties of TGDDM cured with DDS. Firstly, the GIM technique and its parameterisation are outlined followed by a detailed examination of how the beta and glass transitions are dealt with in the model. This section includes an experimental DMTA spectrum for TGDDM/DDS between −100 and 300 °C and the method used to predict equivalent quantities using GIM. This is followed by a full set of predicted properties for TGDDM/DDS leading to a stress–strain curve through yield. Lastly, the strain rate and temperature dependence of the stress–strain curves are examined and compared to experiment.
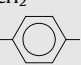
2. Group Interaction Modelling

Group Interaction Modelling (GIM) uses a mean-field potential function approach to predict the structural (thermal, volumetric and mechanical) properties of polymers [2]. The method uses a simple contribution based approach to calculating the total energy of the system. Interactions between neighbouring polymer chains are defined using a potential function that consists of several thermodynamic energy terms. This so-called thermodynamic potential function represents the equation of state for the system as shown in Eq. (1).

$$E_{total} = \phi_0 \left[\left(\frac{V_0}{V} \right)^6 - 2 \left(\frac{V_0}{V} \right)^3 \right] = 0.89 E_{coh} - H_T \qquad (1)$$

The total energy of the system, E_{total}, is expressed as a potential energy well of depth ϕ_0 and is based upon a standard Lennard–Jones function using the volume, V. In bulk model terms, the total energy is comprised of cohesive, E_{coh}, thermal, H_T, and

Table 1
GIM input parameters

	N	E_{coh} (0 K) (J/mol)	V_W (cm³/mol)
CH₂	2	4500	10.25
⬡ (phenylene)	3	25,000	43.3
N	2	9000	4
epoxy (O triangle)	4	15,300	22
CH(OH)	2	20,800	11.5
SO₂	2	45,000	20.3
TGDDM mer unit	36	191,700	232.9
DDS mer unit	12	113,000	114.9

Degrees of freedom, N, cohesive energy at 0 K, E_{coh}(0 K) and van der Waal's volume, V_W. The table shows functional group and uncured mer unit contributions before corrections for cross-linking are made.
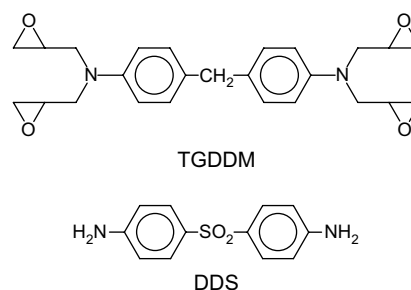

Fig. 1. Chemical structures of tetraglycidyl 4,4′-diaminodiphenylmethane (TGDDM) and 4,4′-diaminodiphenylsulphone (DDS).

configurational contributions. In practice, the configurational energy can be given as a fixed fraction of the cohesive energy which for an amorphous polymer is equal to $0.11E_{coh}$. Eq. (1) represents the energy basis for an amorphous polymer where a balance exists between cohesive and thermal energy contributions. The GIM method uses this energy relation as a basis to derive predictive equations for structural properties. In order to quantify the energy terms, a series of fundamental quantities are required that relate the energy terms to the structure of the polymer.

Several fundamental parameters are required as input into GIM and are based on the representative mer unit. These are the degrees of freedom, N, the cohesive energy at absolute zero, E_{coh}(0 K), the van der Waal's volume, V_W, the length, L, the molecular weight, M, and the Debye temperature, θ_1. The parameters are well defined and constant for each mer unit, though the variation of N with temperature through the two transitions is of importance later. The values of these parameters can be obtained from a variety of sources, including contribution tables [13], connectivity indices [14] or molecular modelling.

The degrees of freedom, N, is the most important of the parameters in GIM and care must be taken in its evaluation. Initial values are taken from group contributions such as those shown in Table 1. The incorporation of cross-linking into the model is ach-ieved by reducing the value of N by 3 for each trifunctional branching site on the mer unit. The fraction of uncross-linked to cross-linked degrees of freedom is used in predicting the charac-teristics of the transitions. Each transition is assigned a specific contribution to the total degrees of freedom based on this fraction and the degree of cure.

For TGDDM cured with DDS, the epoxy and amine are combined in a stoichiometric ratio of 1:1 as both components have 4 reactive sites. The other five input parameters are taken from the functional group contributions in Table 1 and summed to give mer unit values. All the input parameters are evaluated for the epoxy and amine mer units based on their molecular structures as shown in Fig. 1. The parameters for the two components are then combined to give parameters for the cured resin mer unit. The GIM parameters for the cured TGDDM/DDS mer unit are given in Table 2.

Table 2
GIM input parameters for the ideally cured 1:1 TGDDM/DDS mer unit with cross-linking included

Input parameter	Value
N	18
E_{coh}(0 K) (J/mol)	152,350
V_W (cm³/mol)	173.9
L (Å)	14
M	333
θ_1 (K)	550

The terms are defined in the glossary.

3. Beta and glass transitions

In TGDDM/DDS two distinct transition events occur in the dynamic mechanical response. Two associated transition temperatures (T_g and T_β) occur where the degrees of freedom parameter, N, increases in a step-wise manner with increasing temperature. The consequence of these changes is an increase in energy dissipation in the system which needs to be accurately modelled to predict the detailed property profile. This section describes a model for the temperature and rate dependence of each transition and the magnitude of the associated loss peaks. We begin by showing the results of a full temperature range dynamic mechanical experiment for reference purposes.

3.1. Experimental characterisation of beta and glass transitions

The recipe for many industrial formulations of TGDDM cured with DDS requires 26% (by weight) curing agent [15]. This corresponds to a molar fraction of DDS of 38% leaving TGDDM in excess. This non-stoichiometric epoxy/hardener ratio in the mixture gives the most desirable properties in the cured resin. However, stoichiometric ratios of reactants are required for high molecular weight polymers and highly cross-linked networked polymers. As the vast majority of experimental papers on TGDDM/DDS use an excess of epoxy [16], it seems likely that either inefficient network formation, inefficient curing or the known level of impurities in MY721 [17] is interfering. The results in this paper show that GIM predictions for TGDDM/DDS are accurate when using a 1:1 ratio of epoxy to hardener.

DDS (a white powder) has a melting point of 162 °C and is insoluble in TGDDM resin (a viscous yellow liquid) at room temperature. Therefore, 26% by weight DDS was added to the resin which had been preheated to a temperature of 125 °C in an oil bath. Vigorous stirring for 10 min at this temperature ensured a homogeneous and transparent mixture. The epoxy resin was degassed in a preheated vacuum oven at a temperature of 100 °C for 30 min until bubbling was minimized before being cast into slab shaped PTFE moulds. The temperature was raised by 3 °C/min to 130 °C where it was cured for 1 h. The temperature was then raised by 2 °C/min to 180 °C for 2 h before cooling in the oven overnight. The cast samples were cleaned, carefully cut to size ($\sim 8 \times 3 \times 30$ mm) and polished. A DMTA test was performed in tension on a sample with no imperfections using a Metravib Viscoanalyser VA 2000 at a frequency of 1 Hz. The results of this test are shown in Fig. 2.

The loss tangent line provides the most information for comparison with GIM predictions. The low temperature beta transition is centred around -45 °C, is distributed over ~ 200 °C and is still active at room temperature. The higher temperature transitions are assigned to the glass transition at 270 °C and a peak associated with post-curing in the Viscoanalyzer at 230 °C. The latter is common in TGDDM/DDS DMTA spectra and is due to incomplete curing of the system at 180 °C. Spectra of this resin cured to 200 °C do not contain this secondary peak [3]. In contrast, the tensile modulus line is included for completeness but is less useful here as the data has not been corrected for machine compliance. However, it does show an increase around 230 °C which correlates with post-curing at this temperature during the test.

3.2. Modelling the glass transition

The glass transition is due to a sharp increase in intermolecular motion as the polymer chains become capable of independent movement. The relation for the glass transition temperature and its frequency dependence within the GIM framework has been derived in detail elsewhere [2]. The glass transition temperature is predicted in GIM with Eq. (2) using the input parameters, N, $E_{coh}(0\,K)$ and θ_1 and the applied strain rate, r. The characteristic vibrational
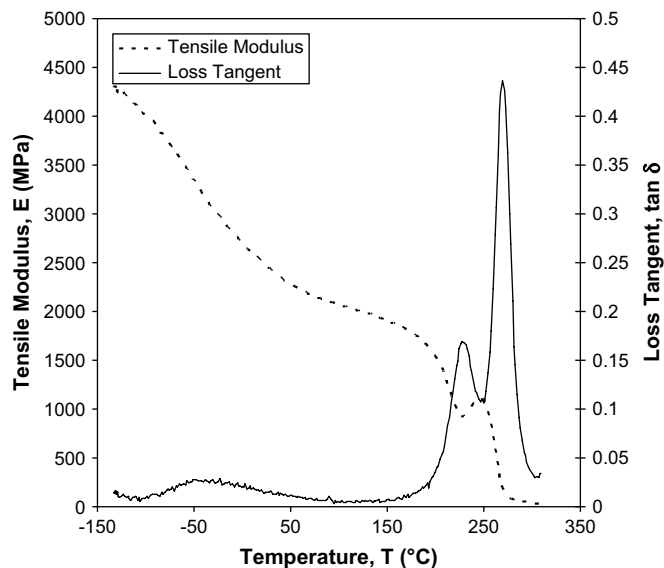

Fig. 2. Experimental DMTA plot for TGDDM/DDS showing tensile modulus (in MPa, dashed) and local loss tangent (solid). A frequency of 1 Hz was used.

frequency of the polymer chain, f is obtained from $k\theta_1 = hf$. Note that we adopt the convention that strain rate is equivalent to angular frequency. Eq. (2) predicts a glass transition temperature for TGDDM/DDS of 281 °C which compares well to the experimental value of 270 °C from in Fig. 2.

$$T_g = 0.224\ \theta_1 + \frac{0.0513 E_{coh}(0K)}{N} - 50 + \frac{1280 + 50\ \ln \theta_1}{\ln\left(\frac{2\pi f}{r}\right)} \quad (2)$$

The cumulative loss tangent through the glass transition, $\tan \Delta_g$, is predicted using Eq. (3) below. Rules for estimating the number of degrees of freedom of the polymer chain, N_c, are defined elsewhere [2]. For TGDDM, $N_c = 50$, and for DDS, $N_c = 30$, which gives $\tan \Delta_g = 32.4$ for TGDDM/DDS.

$$\tan \Delta_g = 0.0085 \frac{E_{coh}(0K)}{N_c} \quad (3)$$

3.3. Modelling the beta transition

The low temperature beta transition is believed to be associated with an intramolecular crankshaft style motion of the phenyl-R-phenyl segments [18]. The exact nature of the low temperature beta transition in epoxy resins is relatively poorly understood and few published works on the subject exist [19]. In modelling terms, all the thermomechanical properties predicted here rely on cumulative quantities such as the total loss tangent to a particular temperature. Hence, it is necessary to model the beta transition fully, considering the fact that most properties of interest are likely to be predicted at temperatures above T_β.

Currently there is no set of equations that predicts the properties of the beta transition based on GIM parameters. To address this issue, the physical processes that cause the beta transition are modelled directly. The beta temperature can be described using an Arrhenius equation as shown in Eq. (4). The activation energy for the beta transition, $-\Delta H_\beta$, is obtained using a simple quantum mechanics routine that estimates the phenyl ring rotation energy in epoxy systems. R is the gas constant, r is the chosen rate and f is the characteristic vibrational frequency of the polymer chain. The beta

transition temperature predicted by Eq. (4) is $-38\,°C$ which compares well with the experimental value of $-45\,°C$ in Fig. 2.

$$T_\beta = \frac{-\Delta H_\beta}{R\,\ln\left(\frac{r}{2\pi f}\right)} \tag{4}$$

Once the position on the temperature scale and rate dependence of T_β are known, the magnitude and distribution of the associated loss peak need to be quantified. The cumulative loss tangent, $\tan \Delta_\beta$, is the area under the loss tangent peak and is used here to quantify the magnitude of the beta event. The loss tangent through the beta transition can be estimated using the ratio of the energy dissipated to the energy stored through an individual beta event [2]. Eq. (5) represents the ratio of energy change (dissipated) as the degrees of freedom increase by ΔN through the transition at T_β to the energy required to go through (stored) the transition over a temperature change, ΔT.

$$\tan \Delta_\beta = \frac{R\,\Delta N T_\beta}{R\,N\Delta T} \tag{5}$$

For TGDDM/DDS, Eq. (5) predicts a value $\tan \Delta_\beta = 3.4$. The shape of the distribution function for $\tan \delta$ cannot easily be expressed in terms of structural parameters. At this stage, the experimental distribution is modelled using two normal distribution peaks (each with standard deviation of about 40 degrees) such that the total area under the curve is $\tan \Delta_\beta$. Two functions are required to model the separate beta loss events in the TGDDM and DDS components. The predicted peak for the beta transition is shown in Fig. 3 along with the experimental peak from Fig. 2. An important point to note for later reference is that a significant fraction of the loss peak occurs above standard observation temperature (e.g. room temperature). This has an effect on the stress–strain properties, as will be shown later.

Fig. 4 shows how the distribution function in Fig. 3 is affected by changing the strain rate in TGDDM/DDS. Note that the distribution width increases linearly with T_β whilst the area under the curve remains constant, as observed experimentally.
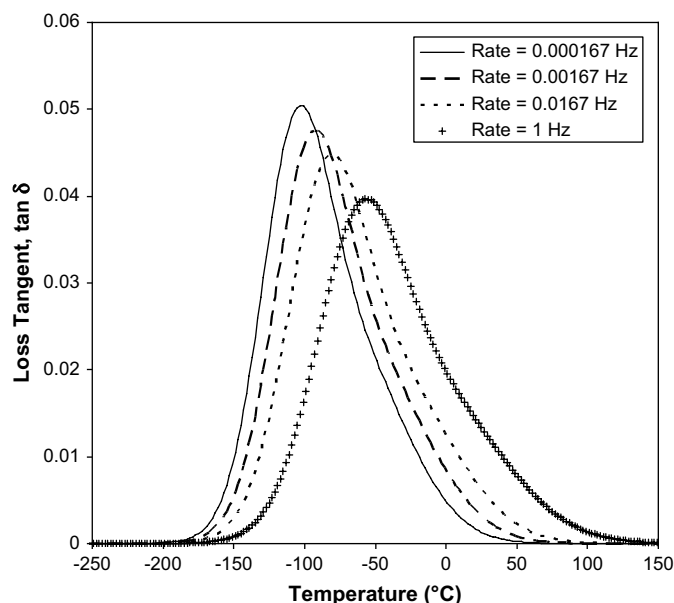
Fig. 4. Predicted variation of the beta transition peak with strain rate for TGDDM/DDS at room temperature.

4. Property prediction

4.1. Volumetric properties

The first step in predicting a full range of thermomechanical properties for cured TGDDM/DDS is the estimation of the energy terms in Eq. (1). The heat capacity of the cured mer unit, C_p, is determined using an empirical approximation to the one-dimensional Debye model as discussed in the extensive experimental work of Wunderlich [20] in Eq. (6).

$$C_p = NR\frac{\left(\frac{6.7T}{\theta_1}\right)^2}{1 + \left(\frac{6.7T}{\theta_1}\right)^2} \tag{6}$$

The heat capacity is integrated to give the thermal energy, H_T, which is plotted against temperature for TGDDM/DDS in Fig. 5. Note that N increases with increasing temperature.

The main change in cohesive energy E_{coh} occurs at the glass transition temperature where its value reduces by approximately 50% due to the significant energy dissipation processes as previously established [2]. Fig. 5 shows the cohesive energy against temperature for TGDDM/DDS. The two plots give an indication of the change in the internal energy balance that exists with rising temperature.

The volumetric properties of the mer unit are predicted via the linear thermal expansion coefficient, α_l, in Eq. (7) which is derived from the temperature derivative of the potential function in Eq. (1).

$$\alpha_l = \frac{1.38C_p}{3RE_{coh}} \tag{7}$$

The expansion coefficient is integrated to give the volume of the mer unit, V, including the van der Waal's volume, V_w, as a factor. The mer unit volume is plotted against temperature for TGDDM/DDS in Fig. 6. The volume of the mer unit can be checked experimentally by comparing the predicted and measured density [3]. Table 3 shows the GIM predicted density and expansion coefficient compare very well with experiment.
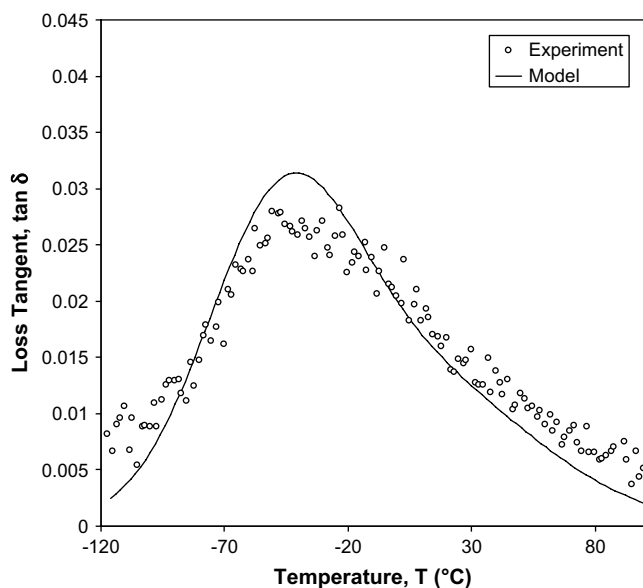

Fig. 3. Comparison between the GIM predicted (solid) and experimental DMTA (points) local loss tangent for TGDDM/DDS. A strain rate of 1 Hz was used at room temperature.
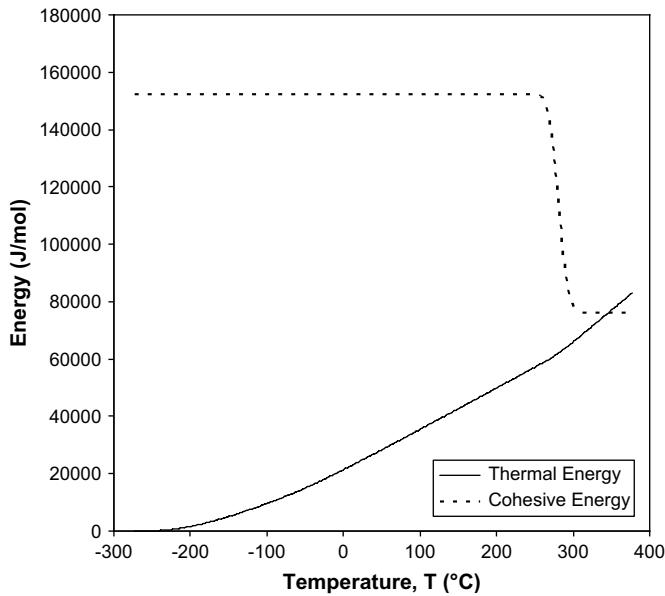
Fig. 5. GIM predicted thermal energy (H_T in J/mol, solid) and cohesive energy (E_{coh} in J/mol, dashed) for TGDDM/DDS. A strain rate of 0.00167 Hz was used at room temperature.

An expression for the elastic bulk modulus, B_e, is obtained by differentiating the potential function in Eq. (1) with respect to volume as shown in Eq. (8).

$$B_e = 18 \frac{E_{total}}{V} \tag{8}$$

The total energy, E_{total}, and volume, V, are the values at the required temperature. The elastic bulk modulus is corrected for the plastic loss associated with both transitions using their cumulative loss tangents. The resulting bulk modulus, B, is plotted against temperature for TGDDM/DDS in Fig. 6 where the two drops centred on T_β and T_g correspond to the two transitions. The beta transition shows a characteristically large temperature range ($\sim 200\ ^\circ$C) while the more dramatic glass transition occurs over a smaller temperature range ($\sim 10\ ^\circ$C).

Table 3
Comparison between predicted and experimental properties for TGDDM/DDS

Property	GIM predicted	Experimental
ρ (g/cm^3)	1.30	1.29
α_l ($\times 10^{-5}$/K)	5	~ 5
E (GPa)	5.17	5.04
σ_y (MPa)	201	200

The density, ρ, (Ref. [3]) and linear thermal expansion coefficient, α_l, (Ref. [25]) are measured at room temperature at a strain rate of 1 Hz. The tensile modulus, E, and the compressive yield stress, σ_y, are taken from Ref. [23].

4.2. Elastic modulus

A new GIM expression for elastic modulus, E, has recently been published [21] which shows a direct relationship between E and the combination of the elastic bulk modulus, B_e and the cumulative loss tangent up to the observation temperature.

$$E = B_e \exp\left(\frac{-\left(\tan \varDelta_g + \tan \varDelta_\beta\right)}{A B_e}\right) \quad \text{where } A = \frac{1.5 \times 10^{-5} L}{\theta_1 M} \tag{9}$$

The elastic modulus in tension, E, is given in Eq. (9) where A is a proportionality constant between elastic modulus and loss tangent in terms of mer unit structural parameters. For TGDDM/DDS, $A = 1.15$ GPa^{-1}.

The predicted tensile modulus is plotted against temperature for TGDDM/DDS in Fig. 7. The tensile modulus varies with temperature in a similar fashion to the bulk modulus, showing the two clear losses at the beta and glass transitions. The predicted modulus at room temperature compares very well to the experimental value given in Table 3. Further comparison of predicted moduli with experiment over a range of temperatures (22–180 $^\circ$C) is given later. It is worth noting that the predicted modulus is in tension while the experimental data used for comparison is in compression. The two values are practically identical at the relatively low strain values used in this work [22]. If the model is extended to incorporate larger strain values then the asymmetry between tension and compression would need to be addressed using a von Mises criterion.
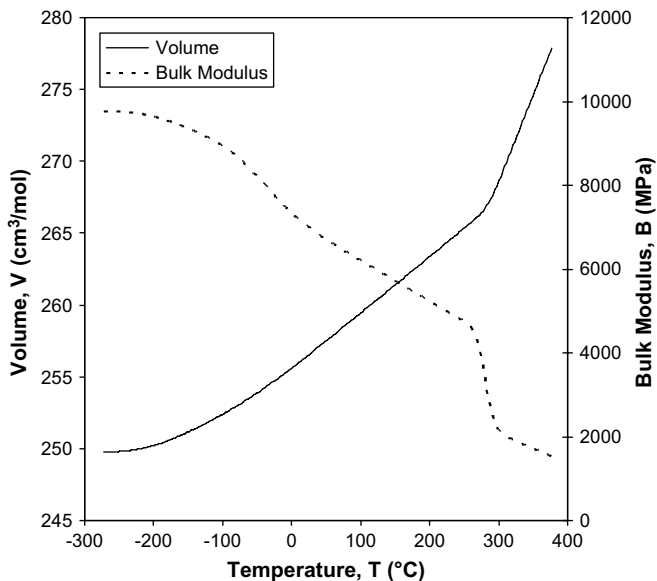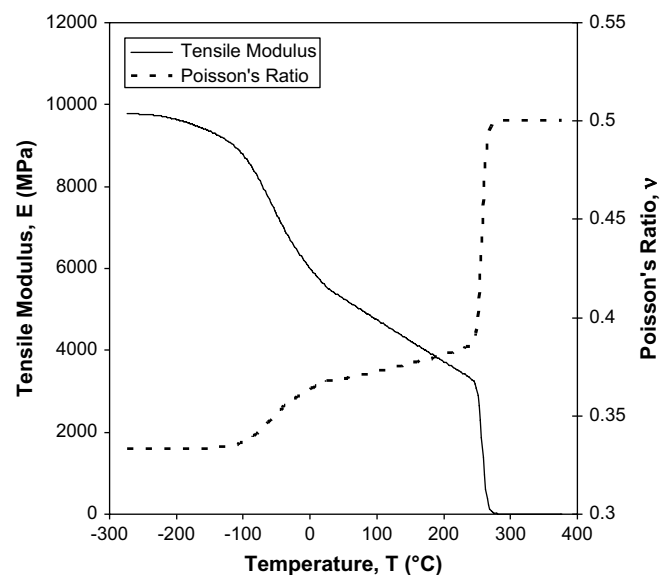

Fig. 6. GIM predicted volume (V in cm^3/mol, solid) and bulk modulus (B in MPa, dashed) for TGDDM/DDS. A strain rate of 0.00167 Hz was used at room temperature.

Fig. 7. GIM predicted tensile modulus (E, in MPa, solid) and Poisson's ratio (ν, dashed) for TGDDM/DDS. A strain rate of 0.00167 Hz was used at room temperature.

The bulk and tensile moduli are combined to give a predicted value of Poisson's ratio, ν, which is plotted against temperature in Fig. 7. The combination of Poisson's ratio and B or E can be used to predict any other modulus parameter. In addition, previous work has suggested that Poisson's ratio can be used to indicate the mode of failure under tension [2]; $\nu < 0.38$ suggests a tendency to brittle failure.

5. Stress–strain curves

In this section, the predicted volumetric and elastic properties are transformed into engineering stress–strain curves. To do this, the elastic and inelastic components of strain need to be quantified. This is done by using the model relations for energy dissipation to scale the elastic strain to include plastic flow effects. In its simplest form, the inelastic contribution to strain is taken to be numerically equal to the cumulative loss tangent up to the observation temperature.

$$\varepsilon = \varepsilon_e \left(1 + \int_0^T \left(\tan \delta_\beta + \tan \delta_g \right) \mathrm{d}T \right) \quad (10)$$

The elastic strain, ε_e, is predicted using the potential function approach by taking strain to be the thermal expansion over a temperature range. In this case, temperature is used as a dummy variable from the observation temperature to an arbitrary maximum value well above T_g. Note the physical identity between the glass transition temperature and the yield point where elastic modulus tends to zero.

$$\varepsilon_e = \int_{T_0}^T \alpha_l \mathrm{d}T \quad (11)$$

From Eqs. (10) and (11), tensile stress is predicted using the elastic modulus over the total strain, again using temperature as a dummy variable.

$$\sigma_t = \int_{T_0}^T E \alpha_I \left(1 + \int_0^T \left(\tan \delta_\beta + \tan \delta_g \right) \mathrm{d}T \right) \mathrm{d}T \quad (12)$$

The compressive stress, σ_c, is calculated with Eq. (13) using a factor 2ν to correct for expansion in the axes normal to the compression axis. Compressive stress is plotted against strain in Fig. 8 for TGDDM/DDS along with an experimental comparison [23].

$$\sigma_c = \frac{\sigma_t}{2\nu} \quad (13)$$

Overall, the GIM predicted stress–strain curve compares very well to the experimental plot. The predicted pre-yield section is very close to experiment including subtle changes in gradient as the yield condition commences. The yield point is then reached at similar values of stress and strain in both the model and experiment. For the purposes of this work, the yield point is defined as the point on the stress–strain curve where the gradient first equals zero. The predicted and experimental yield stress compare very well, as shown in Table 3. The experimental curve includes a period of strain-softening and strain-hardening in the post-yield section. For this class of polymers, the effect is relatively minor and is not included in this work.

In line with existing predictive techniques [24] our model has been specifically developed to allow variation in strain rate and temperature so that comparison to experimental data is as thorough as possible. The GIM prediction of glass and beta transition temperatures via Eqs. (2) and (4) incorporates strain rate variation
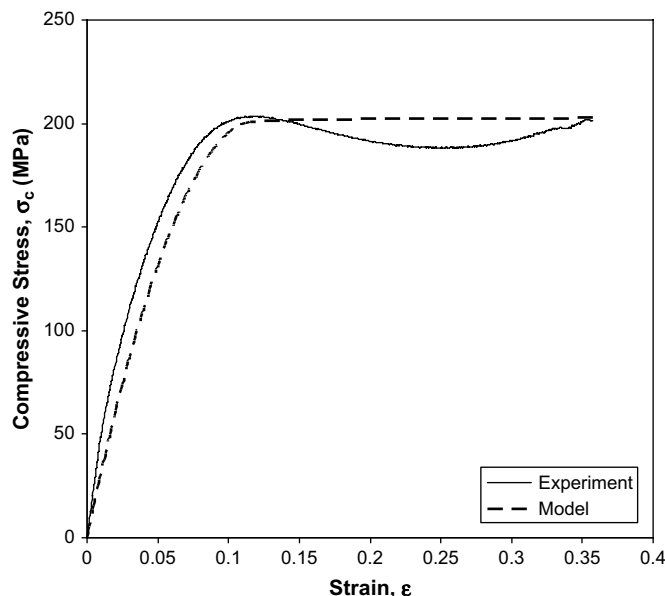

Fig. 8. Comparison between the experimental (solid) and GIM predicted (dashed) compressive stress–strain curve for TGDDM/DDS. A strain rate of 0.00167 Hz was used at room temperature.

via the rate, r. The variation of predicted compressive modulus and yield stress with strain rate is shown in Fig. 9 for TGDDM/DDS. The comparison between model and experiment is good over three different strain rates. While the predicted yield stresses are all within experimental error, there is a discrepancy at the lowest rate modulus value. The model predicts a somewhat larger modulus than is seen experimentally which is thought likely to be due to the onset of creep. Currently, creep is not included in the model though it may be significant at the lower rates.

The variation of modulus and yield stress with temperature is given in Fig. 10 for TGDDM/DDS. Again, the comparison between model and experiment is good. The predicted moduli vary with
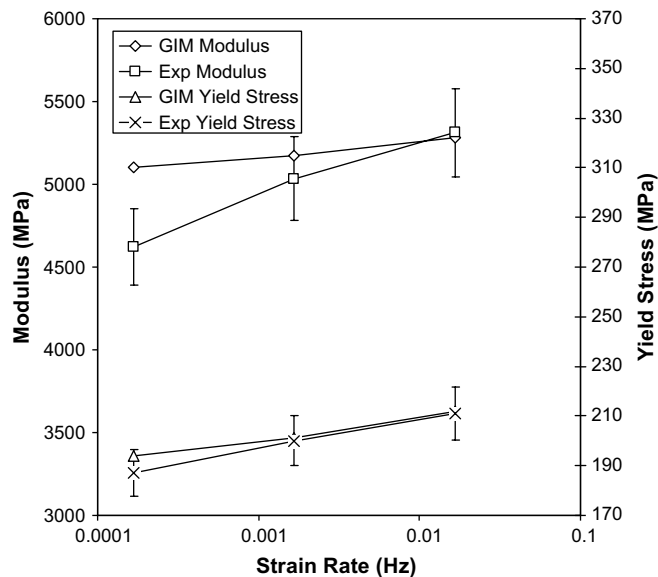

Fig. 9. GIM predicted and experimental room temperature modulus and compressive yield stress (both in MPa) for TGDDM/DDS. Experimental data is taken from Ref. [23]. 5% error bars are included on the experimental points.
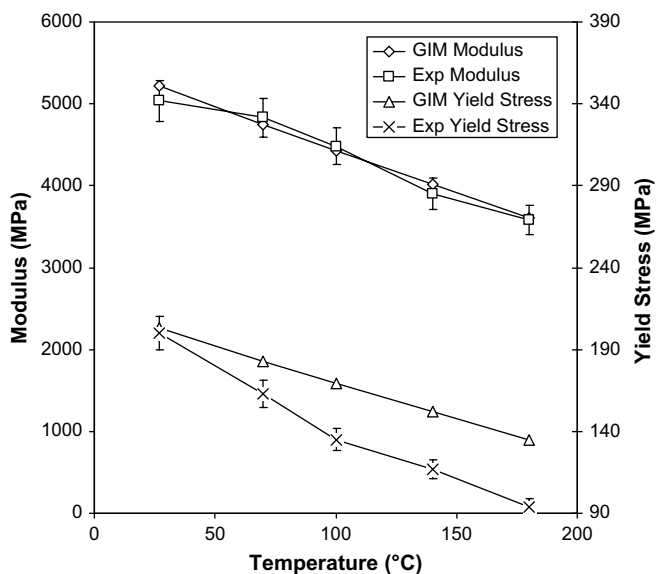
Fig. 10. GIM predicted and experimental modulus and compressive yield stress (both in MPa) for TGDDM/DDS at a strain rate of 0.00167 Hz. Experimental data is taken from Ref. [23]. 5% error bars are included on the experimental points.

temperature almost exactly as they do experimentally. However, the predicted yield stresses appear to suffer from creep effects at higher temperatures and are less accurate.

6. Conclusions

Group Interaction Modelling of polymers which has previously concentrated on linear systems has been revised and extended. It is now capable of predicting the thermomechanical and engineering properties of a highly cross-linking, two-component amine cured epoxy resin system. Moreover, the single property-targeted approach of previous works has been extended so that the model now predicts properties over a full temperature range from fundamental energy contributions right up to moduli and stress–strain curves.

The two transitions in the dynamic mechanical response play a significant role in controlling the properties of the cured resin. The glass transition is already a well defined and parameterised phenomenon but modelling the beta transition required an examination of the physical processes that occur at low temperatures. In addition to this, cross-linking is intrinsically linked to the beta transition via modification of the degrees of freedom. Strain rate dependence is included in the model by predicting the change in the dynamic response of the two transitions.

The predicted properties for the tetrafunctional epoxy resin TGDDM cured with the amine DDS compare very well with experiment. An experimental DMTA plot for TGDDM/DDS over a wide temperature range revealed essential details about the nature of the beta transition. Comparison of the model with strain rate and temperature dependent stress–strain curves shows that the model is capable of predicting a full range of properties to a very good level of accuracy. The model will be applied to a trifunctional epoxy resin in due course followed by resin blends.

Acknowledgments

References

[1] Jones FR. In: Soutis C, Beaumont PWR, editors. Multi-scale modelling of composite material systems. Cambridge: Woodhead; 2005. p. 1–31.
[2] Porter D. Group interaction modelling of polymer properties. New York: Dekker; 1995.
[3] Foreman JP, Porter D, Behzadi S, Travis KP, Jones FR. J Mater Sci 2006;41:6631.
[4] Gumen VR, Jones FR, Attwood D. Polymer 2001;42:5717.
[5] Lesser AJ, Calzia KJ. J Polym Sci Part B Polym Phys 2004;42:2050.
[6] Calzia KJ, Lesser AJ. J Mater Sci 2007;42:5229.
[7] Epoxy resins. In: Encyclopedia of polymer science and technology, vol. 9. Wiley; 2002.
[8] Gupta A, Cizmecioglu M, Coulter D, Liang RH, Yavrouian A, Tsay FD, et al. J Appl Polym Sci 1983;28:1011.
[9] Foreman JP, Porter D, Behzadi S, Jones FR, in preparation.
[10] Foreman JP, Behzadi S, Porter D, Curtis, PT, Jones FR. J Mater Sci, doi:10.1007/s10853-008-2688-9.
[11] Behzadi S, Curtis PT, Jones FR. In: Proceedings of ICCM-16, Kyoto; 2007.
[12] Curtis PT. Compos Sci Technol 1986;27:63.
[13] Van Krevelen DW. Properties of polymers. Amsterdam: Elsevier; 1993.
[14] Bicerano J. Prediction of polymer properties. New York: Dekker; 1993.
[15] Serrano D, Harran D. Eur Polym J 1988;24(7):667.
[16] (a) Moy P, Karasz FE. Polym Eng Sci 1980;20(4):315;
    (b) Morgan RJ, O'Neal JE, Fanter DL. J Mater Sci 1980;15(3):751;
    (c) Stark EB, Seferis JC, Apicella A, Nicolais L. Thermochim Acta 1984;77 (1–3):19;
    (d) Apicella A, Nicolais L, Iannone M, Passerini P. J Appl Polym Sci 1984;29(6):2083;
    (e) Mijovic J, Kim J, Slaby J. J Appl Polym Sci 1984;29(4):1449;
    (f) St. John NA, George GA, Cole-Clarke PA, Mackay ME, Halley PJ. High Perform Polym 1993;5:21;
    (g) Halley PJ, Mackay ME, George GA. High Perform Polym 1994;6:405;
    (h) Barral L, Cano J, Lopez J, Nogueira P, Ramirez C, Abad MJ. Polym Int 1997;42(3):301;
    (i) Zhou J, Lucas JP. Polymer 1999;40(20):5505;
    (j) Musto P, Mascia L, Ragosta G, Scarinzi G, Villano P. Polymer 2000;41(2):565;
    (k) Cotugno S, Larobina D, Mensitieri G, Musto P, Ragosta G. Polymer 2001;42(15):6431.
[17] St. John NA, George GA. Prog Polym Sci 1994;19(5):779.
[18] Williams JG. J Appl Polym Sci 1979;23:3433.
[19] Robeson LM, Farnham AG, Mcgrath JE. In: Molecular basis of transitions and relaxations. New York: Gordon and Breach; 1978.
[20] Wunderlich B, Cheng SZD, Loufakis K. Encyclopedia of polymer science and engineering, vol. 16. New York: Wiley; 1989.
[21] Porter D, Vollrath F, Shao Z. Eur Phys J E 2005;16:199.
[22] Kozey VV, Kumar S. J Mater Res 1994;9(10):1994.
[23] Behzadi S, Jones FR. J Macro Sci Part B Phys 2005;44:993.
[24] (a) Richeton J, Ahzi S, Vecchio KS, Jiang FC, Makradi A. Int J Solids Struct 2007;44:7938;
    (b) Richeton J, Ahzi S, Vecchio KS, Jiang FC, Adharapurapu RR. Int J Solids Struct 2006;43:2318.
[25] Caballero-Martinez MI. Ph.D. thesis, University of Sheffield; 2004.

Glossary

A: Loss factor
B_e: Elastic bulk modulus
C_p: Heat capacity
E: Tensile modulus
E_{total}: Total GIM energy
E_{coh}: Cohesive energy
$E_{coh}(0\,K)$: Cohesive energy at 0 K
f: Characteristic vibrational frequency of the polymer chain
H_T: Thermal energy
ΔH_β: Activation energy of the beta transition
h: Planck's constant
k: Boltzmann's constant
L: Length of the mer unit
M: Molecular weight of the mer unit
N: Degrees of freedom
N_c: Degrees of freedom of the polymer chain
ΔN: Degrees of freedom change for a single beta event
R: Gas constant
r: Strain rate
T: Temperature
T_g: Glass transition temperature
T_β: Beta transition temperature
ΔT: Temperature change for a single beta event
$\tan \Delta_\beta$: Cumulative loss tangent through the beta transition

tan Δ_g: Cumulative loss tangent through the glass transition
V: Volume of the mer unit
V_w: van der Waal's volume of the mer unit
α_l: Linear thermal expansion coefficient
ε_e: Elastic strain
ε: Strain

ν: Poisson's ratio
θ_1: Debye temperature normal to polymer chain axis
ρ: Density
σ_c: Compressive stress
σ_t: Tensile stress
σ_y: Compressive yield stress